

Investigation of the Plunging Pressure Pulsation in a Swirling Flow with Precessing Vortex Rope in a Straight Diffuser

S Muntean^{1,3}, C Tănasă², A I Bosioc² and D C Moş²

¹ Romanian Academy – Timișoara Branch, Bv. Mihai Viteazu, No. 24, Timisoara, Romania

² Politehnica University Timișoara, Bv. Mihai Viteazu, No. 1, Timisoara, Romania

E-mail: seby@acad-tim.tm.edu.ro

Abstract. The paper investigates an unexpected feature of the unsteady pressure field resulting from the self-induced instability of the decelerated swirling flow in a straight diffuser. Firstly, the self-induced instability is experimentally investigated on the swirl generator test rig. As a result, the asynchronous (rotating) pressure pulsation associated with the rotating vortex rope of 15 Hz and its second harmonic are discriminated. Also, a low frequency synchronous (plunging) pulsation around of 2.5 Hz is identified based on unsteady pressure field measured at the wall and LDV measurement of the velocity components in the flow. The low frequency plunging pressure fluctuations are superimposed on the rotating pressure pulsations associated with the vortex rope. The numerical simulations are performed to explore the vortex rope dynamics. The numerical results are compared against experimental data to assess the accuracy of the models. Next, the pressure pulsation dynamics is correlated with the time evolution of the vortex rope. The main conclusion emerging from the analysis of the vortex rope evolution in time is that the cycle with low frequency is responsible for the plunging (synchronous) pressure fluctuations superimposed over the rotating (asynchronous) pressure field associated with the precession of the vortex rope.

1. Introduction

The large pressure fluctuation in the draft tube of a Francis turbine at part-load operation is called draft tube surge by Rheingans [1]. This phenomenon is extensively investigated during last five decades in order to elucidate its mechanism [2-5]. Then, several solutions have been proposed to mitigate its effects [6]. A synopsis outlook about these investigations and solutions are presented by Nishi and Liu [7].

The group coordinated by Prof. Nishi [3] has shown that the pressure pulsation consists of a synchronous part (plunging) and an asynchronous part (rotating), respectively. Moreover, he has conducted experimental investigations which proved that the synchronous pulsation does not exist in a straight draft tube. As a result, he stated that the synchronous component resides in the elbow.

Dörfler et al. [8, Ch. 2] review the whole range of low-frequency phenomena in swirling flows, with particular emphasis for hydraulic turbines. The Nishi's idea is adopted by Dörfler et al. [8, §2.2.11.2] to explain the physical mechanism that produces the plunging pressure pulsation with low-frequency in swirling flow.

³ To whom any correspondence should be addressed



Recently, Stuparu and Susan-Resiga [9] claimed that the plunging pressure pulsation is an intrinsic feature of the helical vortex dynamics. Their statement is based on unsteady turbulent flow simulation performed in a three-dimensional axis-symmetric surrogate draft tube. As a result, the plunging oscillations are not necessarily the result of the interaction between the vortex rope and the draft tube elbow as was stated by Prof. Nishi.

Both cases were distinguished within our experimental investigations performed on the swirling flow test rig developed at Politehnica University of Timisoara. At some hydrodynamic conditions, a low frequency plunging component is discriminated in the swirling flow only if the elbow is installed downstream to the test section. At other hydrodynamic conditions, a distinct low frequency plunging component than the previous one is evidenced in the swirling flow of the straight diffuser without any elbow. Particularly, both plunging components with low frequencies are identified in the swirling flow when the hydrodynamic conditions correspond to the second case and the elbow is installed downstream to the test section.

In this paper, our experimental and numerical investigations are presented in order to examine the cause of low frequency plunging oscillations in a straight diffuser. The experimental setup is described in Section 2 together with Fourier spectra obtained on the wall at five levels of the test section with straight diffuser. Also, the Fourier spectra for two points located on test section axis are determined using LDV system in order to be identified the dominant frequency of the unsteady velocity field. The computational domain and numerical setup are presented in Section 3. The numerical results obtained with three turbulence models are compared against experimental data in order to assess its capability to capture the plunging and rotating components. The helical vortex dynamics is numerically investigated, in Section 4, in order to elucidate the cause of plunging oscillations in a straight diffuser. The conclusions are drawn in the last section.

2. Experimental setup/data

2.1. Experimental setup

The test rig is designed to investigate several swirling flow configurations. Several swirling flow configurations are generated using two strategies: (i) different guide vane geometries are designed and tested together with a free runner [10, 11]. The speed of free runner is modified from one geometry to another providing different swirling flow configuration: (ii) the runner speed is slow down using a magneto-rheological device [12, 13]. These swirling flow configurations correspond to hydrodynamic conditions associated to Francis turbine operation [12-14].

The test rig is equipped with an acquisition system in order to record the discharge and runner speed [15]. The most important part of the rig is the test section, Fig. 1a. The test section includes the swirl apparatus with two rows of blades (13 guide vanes and 10 runner blades) [16] and the convergent-divergent section [17]. The test section is manufactured from plexiglass in order to allow flow visualization. The throat diameter is 100 mm while the conical diffuser has a 8.5° half-angle and 200 mm in length.

Two test sections were manufactured, Fig. 1. The first one allows us to measure the unsteady pressure on the cone wall at four levels using eight transducers, see Fig. 1b. As a result, two pressure transducers are installed on each level being positioned at 180° each other. The first level corresponds to the throat (MG0) and the next levels are displaced at 50 mm (MG1), 100 mm (MG2) and 150 mm (MG3) with respect to the first one. One more transducer is flush mounted on the wall of the upstream cylindrical part of the test section, see Fig. 1a. The position of the upstream pressure transducer is 400 mm with respect to the throat (MG0) level. The transducers measurement range was ± 1 bar with a precision of $\pm 0.13\%$. However, the upper limit of frequency for unsteady pressure transducers is beyond to 50 Hz. The second section is designed to measure along to three survey axis (W0, W1 and W2) using a LDV system with two velocity components (Fig. 1c) and the unsteady pressure at two levels (MG0 and MG2) using Kistler fast response transducers.

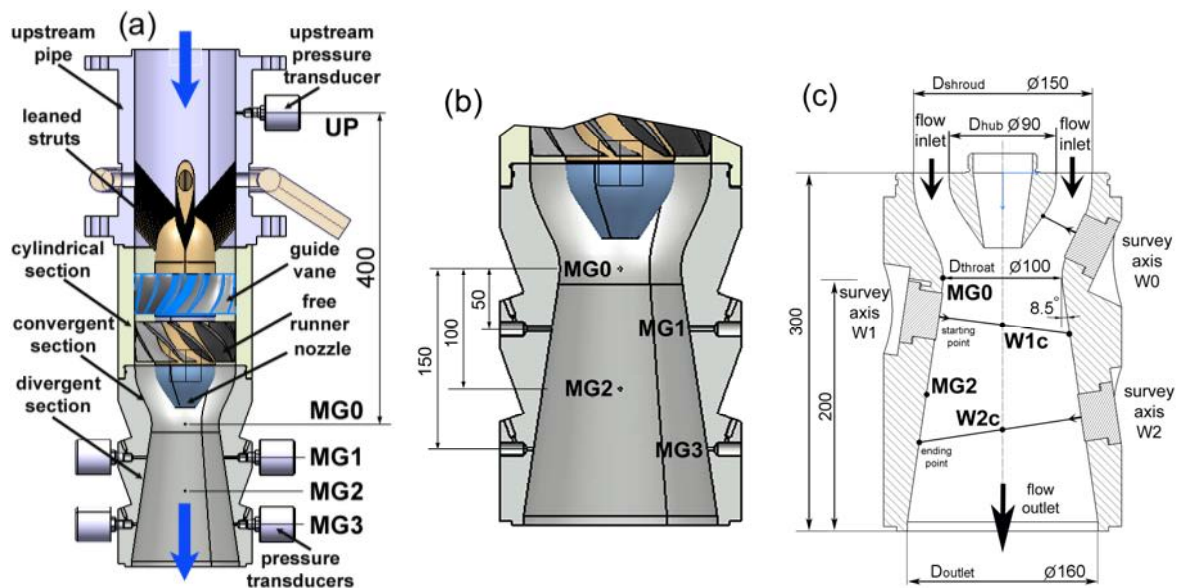


Fig. 1 Meridian cross-section of the test section (a), zoom-up of the convergent-divergent test sections with pressure taps (b) and LDV windows (c).

In our investigations a nominal discharge of 30 l/s is selected. In this case, the swirling flow configuration provided by the stay vanes leads to a free runner speed of 920 rpm. In this paper only the swirling flows under non-cavitating conditions are performed.

2.2. Experimental data analysis

Firstly, the Fourier spectrum of the signal recorded by the pressure transducer (UP) located upstream to the test section (see Fig. 1a) is plotted in Fig. 2. The discriminated signals cannot be obtained on this level due to only one transducer is installed. Two frequencies around 2.5 Hz and 19 Hz can be clearly identified at this level.

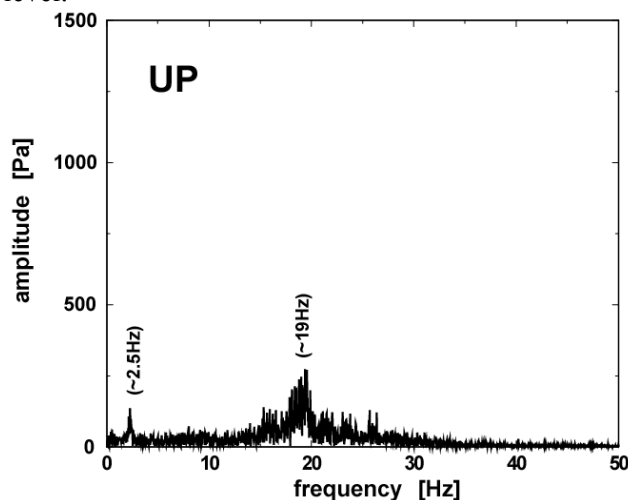


Fig. 2 Fourier spectrum of the unsteady pressure signal acquired by the pressure transducer (UP) located upstream to the test section, see Fig 1a.

Secondly, two unsteady pressure signals acquired on each four level of the cone are used to discriminate the plunging and rotating components using the procedure proposed by Nishi et al [3, 9]. The Fourier spectra of the decomposed signals are plotted in Fig. 3. Further, the spectrum of the plunging component (PC) is shown with black while the spectrum of the rotating one (RC) with red, respectively.

One can observe on the Fourier spectrum of the rotating component that the vortex rope frequency is around 15 Hz. The largest amplitude of the rotating component is measured on MG2 level. The amplitude of the rotating component is ten times smaller on MG3 level with respect to MG2 level. The frequency of 30 Hz is distinguished on the Fourier spectrum of the rotating component on the levels MG1 and MG2. This frequency corresponds to second harmonic of the vortex rope ($30 \text{ Hz} = 2 \times 15 \text{ Hz}$). The largest amplitude of this frequency is assessed on MG2 level being the same level with rotating component. It is obvious that these two frequencies are connected with the vortex rope. The rotating component is generated by the vortex rope and it remains trapped in the cone [5].

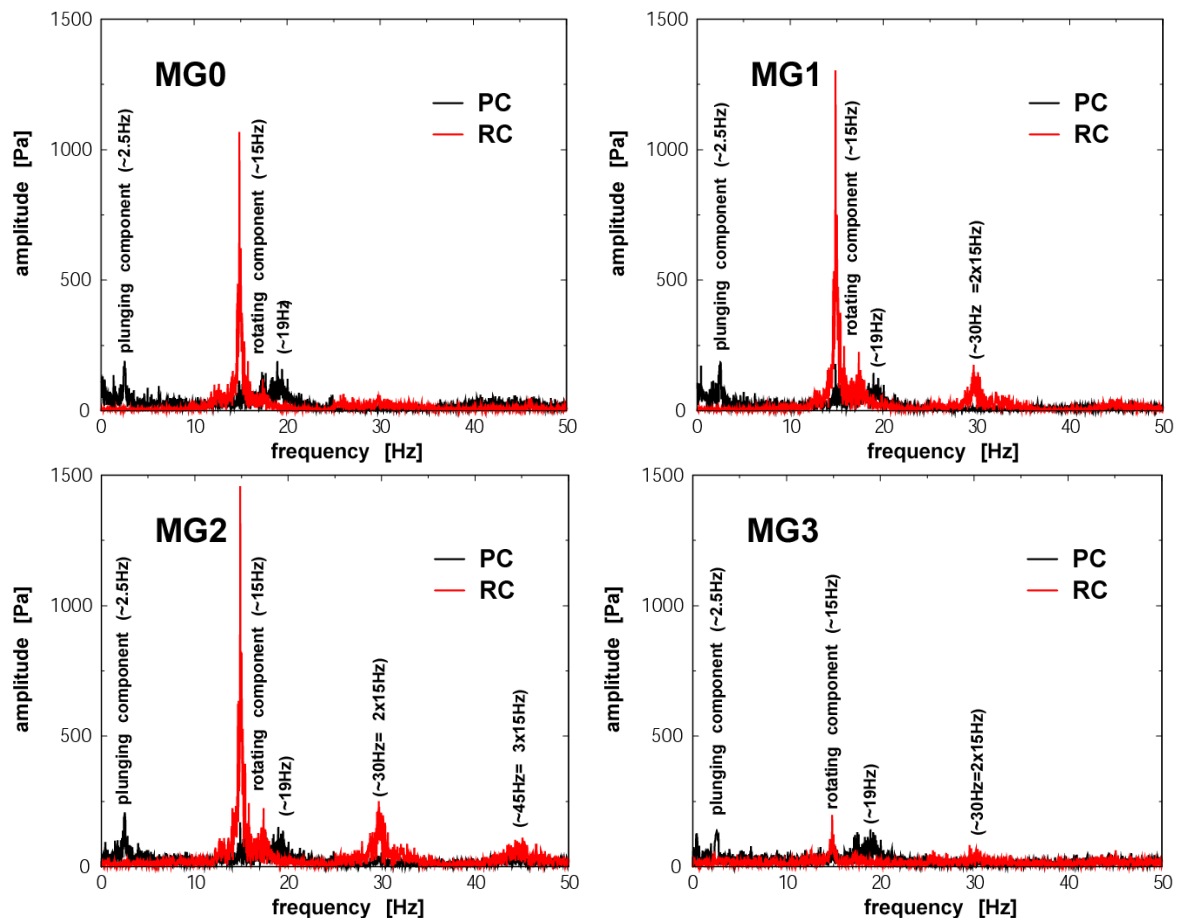


Fig. 3 Fourier spectra of the decomposed unsteady pressure signals at all four levels on the cone wall (from MG0 to MG3, Fig. 1b).

Two frequencies around 2.5 Hz and 19 Hz can be distinguished on the plunging component of the Fourier spectra. The low frequency around 2.5 Hz is clearly observed on all levels displaced in the cone (from MG0 to MG3) and upstream. The largest amplitude is determined in the cone and the smallest one on the upstream level. It is assumed that this frequency originates in the cone based on above observation.

The frequency around 19 Hz is observed on all levels along to the test section. The largest amplitude is obtained on the upstream level while the smallest one on MG3 level. Therefore, it is expected that this frequency to be associated to the test rig being generated upstream to the test section and it is propagated downstream. However, all above spectra are obtained using signals recorded at the wall. Next, LDV system with two components is used to check if previous frequencies can be identified within the unsteady flow field. In this case, two monitors (W1c and W2c, see Fig. 1c) located on the test section axis are selected to check the occurrence of the low plunging component.

The Fourier spectra of the signals acquired in these two monitors are plotted in Fig. 4. One can observe that the low plunging component of 2.5 Hz is stronger in the first part of the cone than the second part. Conclusively, our experimental investigation within a straight diffuser clearly reveals a low synchronous (plunging) pulsation and the source of it is located in the first part of the cone.

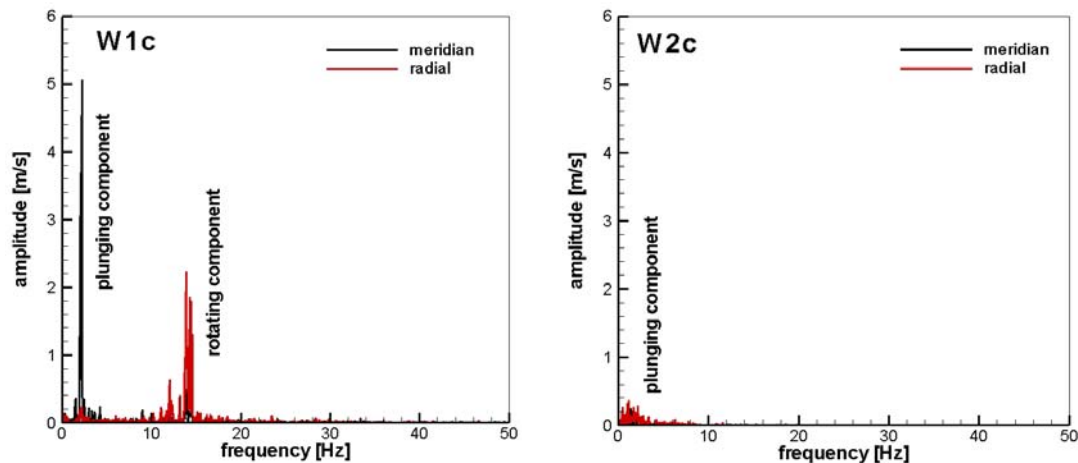


Fig. 4 Fourier spectra of the unsteady velocity component signals acquired in two locations on the test section axis: W1c and W2c (see Fig. 1c)

3. Numerical setup/data

The 3D numerical investigations are performed in order to elucidate the cause of the low plunging component. The numerical setup is presented followed by the validation of the numerical results against experimental data.

3.1. Numerical setup

The 3D computational domain corresponds to the convergent-divergent section of the test rig, Fig. 5. The inlet boundary conditions are imposed on the annular section located just downstream to the free runner while the outlet section belongs to a cylindrical extension of the divergent part, see Fig. 1.

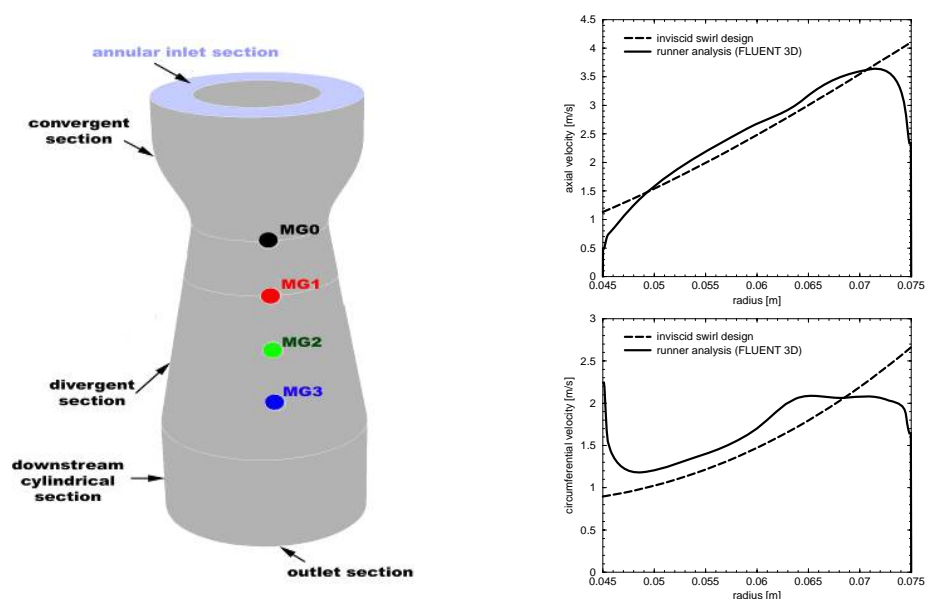


Fig. 5 3D computational domain with pressure taps marked on the conical section and the velocity profiles imposed as inflow conditions.

Fig. 5 shows the inviscid design of the swirl just downstream the runner (dashed lines) and the actual velocity profiles yielded from a turbulent 3D numerical analysis of the flow in the runner (solid lines) [14]. Although the axial velocity closely follows the intended profile, the circumferential velocity cannot reach the intended profile near the shroud. However, this 3D turbulent velocity profile is used as inflow condition in our numerical computations, together with profiles of turbulence kinetic energy and dissipation from the same numerical results [18].

The numerical simulations presented in this work were done with FLUENT 6.3 [19]/16.2 codes [20]. A structured mesh with 2 million cells is used. The average y^+ values range between 40-240, except in the separated region below the central body, where it increases to 400, but in that region the log-law does not make sense anyway. The unsteady Reynolds-averaged Navier-Stokes equations with three turbulence models closure are considered. The RNG $k-\epsilon$ model is selected together with enhanced wall treatment and pressure gradient effects. The radial equilibrium condition was used at the outlet based on previous validation [18].

The convection terms are discretized using a 2nd order scheme, and the time terms are discretized using the 2nd order scheme for numerical stability. The time step was selected 10^{-4} s based on numerical study performed to capture as accurate as possible the frequency of the rotating component [21].

3.2. Numerical results. Validation against experimental data

Although the computational domain is axi-symmetric, Fig. 5, and the inlet boundary conditions are steady and axi-symmetric (radial profiles for axial and circumferential velocity components), the decelerated swirling flow in the conical diffuser develops an instability with a precessing helical vortex [18, 22] as shown in Fig. 6 with a low frequency component embedded in it [23, 24].

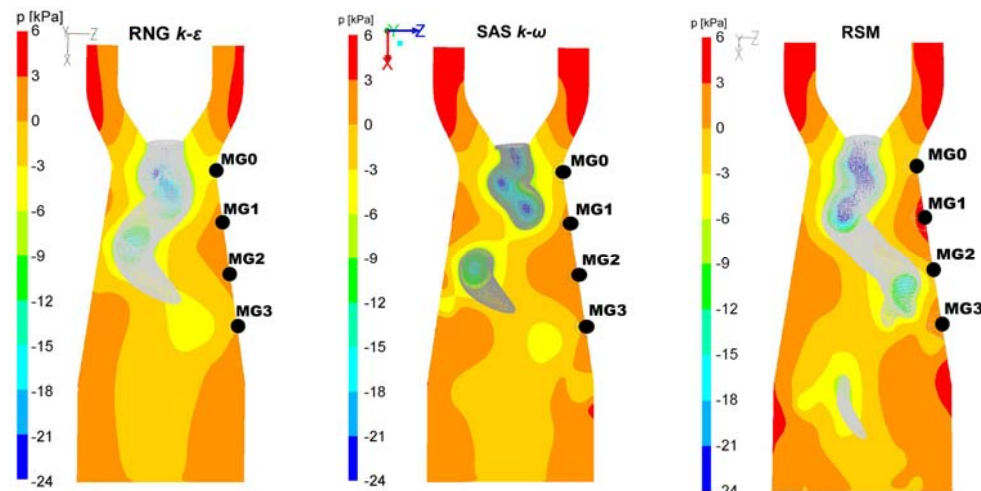


Fig. 6 The vortex rope is visualized based on numerical simulation with three models (RNG $k-\epsilon$ model, SAS $k-\omega$ model and RSM model) using iso-pressure surface.

All turbulence models considered in this paper are able to reproduce the well-known precessing vortex rope visualized on the test rig. The vortex rope is visualised for all turbulence models in Fig. 6 using a snapshot of an iso-surface of static pressure. The meridian cross-section is colored by the static pressure. Both RNG $k-\epsilon$ and SAS $k-\omega$ models are able to reproduce the vortex rope development situated in the first part of the cone. However, both models are limited to capture the vortex rope tail located in the second part of the cone with respect to the RSM model.

This three-dimensional precessing helical vortex induces an unsteady pressure field. Four numerical pressure monitors (from MG0 to MG3) are located along to the element of the cone in the same positions as the pressure taps in the experimental setup, see Fig. 1. The numerical results are validated against experimental data in order to assess the numerical set-up. The Fourier spectra on MG0 and MG2 levels

are presented in Fig. 7. The numerical simulation with RNG $k-\varepsilon$ model captures well both frequency and amplitude of the rotating component on MG0 level while its amplitude is overestimated on MG2 level. Moreover, this model is not able to capture any plunging component [18].

The SAS $k-\omega$ model provides an improved prediction of the unsteady hydrodynamic field than RNG $k-\varepsilon$ model. The frequency of the rotating component is accurately restored by the SAS $k-\omega$ model on both levels while the amplitude is underestimated on MG0 level. Contrary, the higher harmonics on MG2 level are overestimated with respect to the experimental data. The low frequency plunging component is captured on both levels with this model.

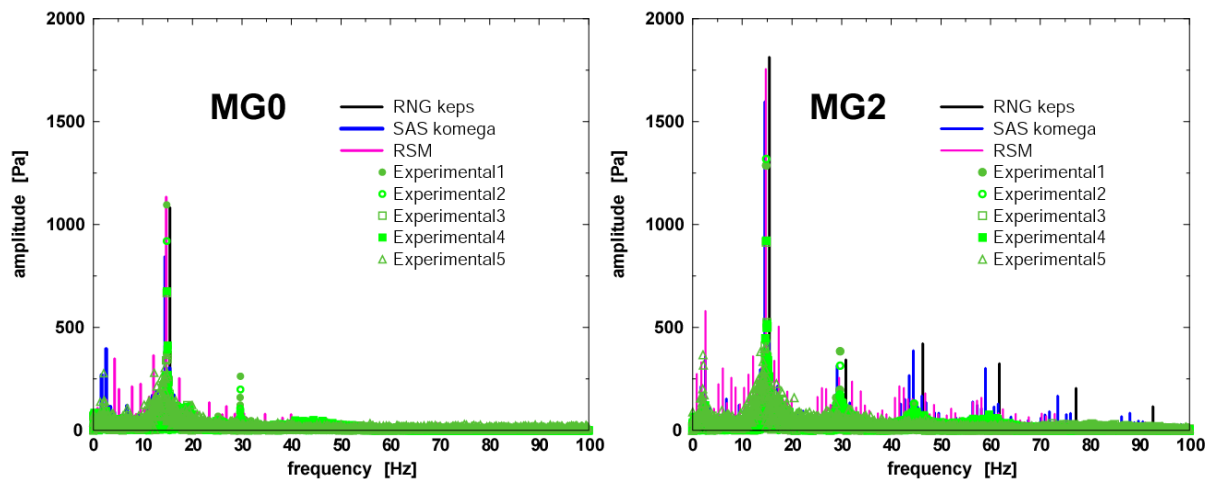


Fig. 7 Validation of the numerical results against experimental data using Fourier spectra of the unsteady pressure signals acquired at MG0 and MG2 levels

Both frequency and amplitude of the rotating component are accurately computed by the RSM model on both levels excepting the amplitude on MG2 level which is overestimated. One can observe an improved prediction for the higher harmonics on MG2 level than numerical results obtained with SAS $k-\omega$ model. Also, the low frequency plunging component is captured on both levels with this model even if an over prediction can be observed on MG2 level. Conclusively, the most accurate numerical results against experimental data are obtained with RSM model. As a result, the RSM model is further used in order to investigate the vortex rope dynamics.

4. Vortex rope dynamics

The vortex rope dynamics in a straight diffuser is explored using the numerical results obtained with RSM model in order to elucidate the cause of the plunging pulsation with low frequency. The unsteady pressure signals recorded during numerical simulation at all four levels are plotted in Fig. 8. It can be easily distinguished on the unsteady pressure signal at MG0 level that a low frequency around 2.5 Hz (1/0.4s) is superposed on a higher frequency around 15 Hz (6 periods associated to higher frequency correspond to 1 period of the low frequency of 2.5 Hz). The previous procedure can be straightforwardly implemented on the unsteady pressure signals recorded on MG1 and MG2 levels. Contrary, it is rather difficult to be applied this procedure on the unsteady pressure signal recorded on MG3 level due to the time periods associated to the frequency of 15 Hz are not so easily detected.

The analysis of the vortex rope morphology during a low frequency period is performed in order to examine its dynamics. As a result, eighty snapshots with a time step of 0.005s are collected during a low frequency period of 0.4s. All these snapshots are marked with red circles in Fig. 8 on recorded signals at all four levels. However, only six snapshots at 3.1, 3.22, 3.275, 3.35, 3.4 and 3.5 seconds (marked with blue spots in Fig. 8) are selected in this paper in order to reveal the time evolution of the vortex rope. The same iso-pressure surface is plotted for these time steps in Fig. 9.

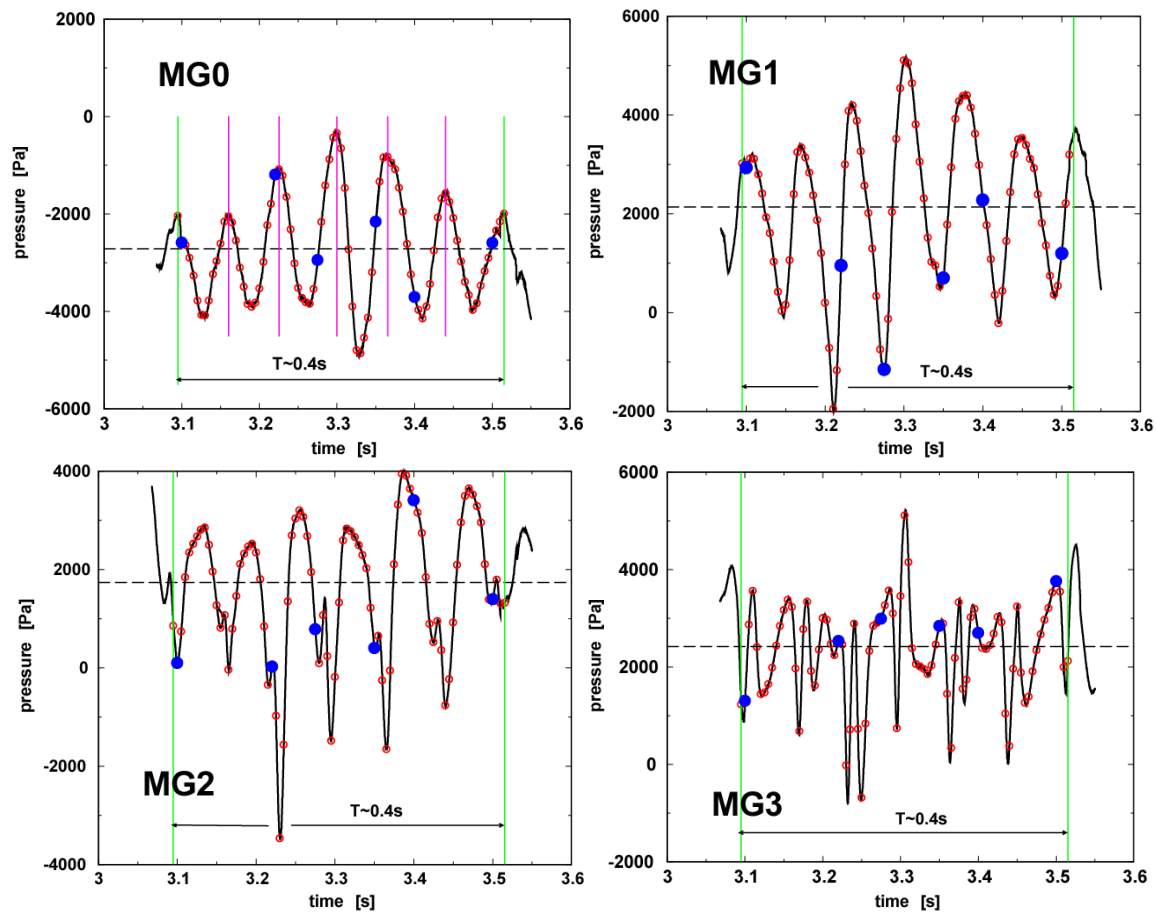


Fig. 8 Unsteady pressure signals recorded at all four levels on the cone (from MG0 to MG3, see Fig. 6) based on 3D numerical simulation with RSM model.

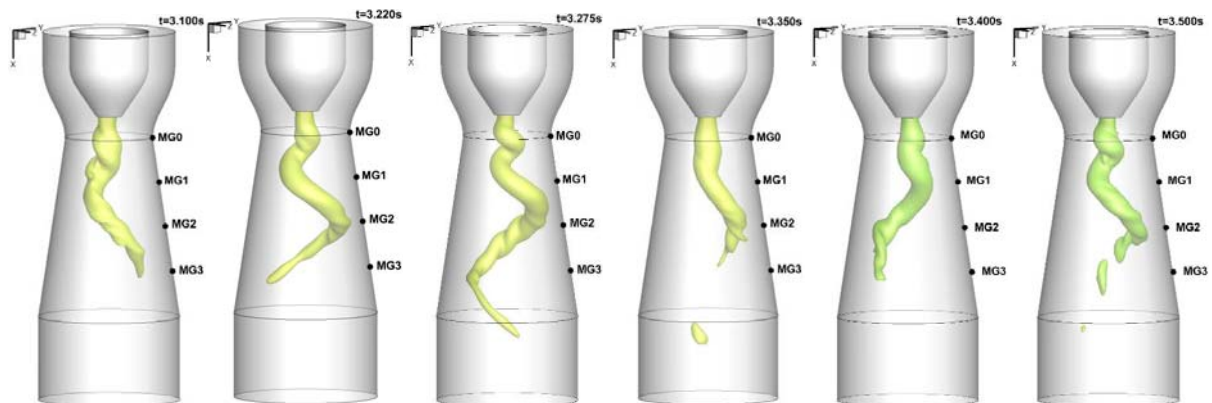


Fig. 9 Morphology of the vortex rope at several time steps obtained from 3D numerical simulation using iso-pressure surface. The snapshots correspond to six time steps (3.1, 3.22, 3.275, 3.35, 3.4 and 3.5 s) marked with blue spots in Fig. 8.

One can observe that the vortex rope is compressed during the first phase of the low frequency cycle. After that the vortex is stretching, leading to an elongated rope, followed by a bouncing back phase. The vortex rope can be imagined like a conical spring with variable helix angle. The cycle with low frequency is responsible for the plunging (synchronous) pressure fluctuations superimposed over the rotating (asynchronous) pressure field associated with the precession of the vortex rope.

Conclusively, the cause of the low plunging (synchronous) pressure component in a straight diffuser at particular hydrodynamic conditions is the self-excitation of the vortex rope instability.

5. Conclusions

In this paper, an unexpected feature of the unsteady pressure field resulting from the self-induced instability of the decelerated swirling flow in a straight diffuser is investigated. Firstly, the self-induced instability is experimentally investigated on the swirl generator test rig. The following data are identified measuring the unsteady pressure at the wall: (i) asynchronous (rotating) pressure pulsation of 15 Hz associated with the rotating vortex rope and its second harmonic; (ii) a low frequency synchronous (plunging) pulsation around 2.5 Hz and a plunging component around 19 Hz, respectively. The Fourier spectra for two points located on test section axis are determined using LDV system in order to be identified the dominant frequency of the unsteady velocity field. A significant plunging component with low frequency around 2.5 Hz is captured on the meridian velocity component in the first part of the cone. Secondly, the numerical simulation of the decelerated swirling flow in a straight diffuser is conducted to elucidate the cause of the low frequency. Three numerical models (RNG k- ϵ , SAS k- ω and RSM) are considered in our investigation. The numerical results are qualitatively and quantitatively validated against experimental data in order to assess the accuracy of the models. The features of the unsteady field are better captured using RSM model. As a result, the vortex rope dynamics is examined considering the unsteady numerical results obtained with this model. It can be easily distinguished on the signal at MG0 level that a low frequency around 2.5 Hz (1/0.4s) is superposed on a higher frequency around 15 Hz (6 periods associated to higher frequency correspond to 1 period of the low frequency of 2.5 Hz). A deep analysis of the vortex rope morphology during a low frequency period is performed in order to examine its dynamics. As a result, eighty snapshots with a time step of 0.005s are collected during a low frequency period of 0.4s. Six snapshots at 3.1, 3.22, 3.275, 3.35, 3.4 and 3.5 seconds (marked with blue spots in Fig. 8) were selected in order to reflect the time evolution of the vortex rope plotting the same iso-pressure surface. The pressure pulsation dynamics is correlated with the time evolution of the pressure surface. It was observed that the vortex rope is compressed during the first phase of the low frequency cycle. After that the vortex is stretching, leading to an elongated rope, followed by a bouncing back phase. The main conclusion emerging from the analysis of the vortex rope evolution in time is that the cycle with low frequency is responsible for the plunging (synchronous) pressure fluctuations superimposed over the rotating (asynchronous) pressure field associated with the precession of the vortex rope.

Acknowledgements

Dr. Muntean S. and Dr. Bosioc. A.I. acknowledge the support from Romanian National Authority for Scientific Research and Innovation, CNCS - UEFISCDI, project number PN-II-ID-PCE-2012-4-0634. Dr. Tănasă C. and Mr. Moş. D.C. have been supported by a grant of the Romanian National Authority for Scientific Research and Innovation, CNCS - UEFISCDI, project number PN-II-RU-TE-2014-4-0489.

References

- [1] Rheingans W J 1940 Power swings in hydroelectric power plants, *Trans ASME* **62** 174 171-184
- [2] Nishi M, Kubota T, Matsunaga S and Senoo Y 1984 Surging characteristics of conical and elbow-type draft tubes, in *Proc. of the 12th IAHR Symp. Section on Hydraulic Machinery, Equipment and Cavitation (Stirling, UK)* 272-283
- [3] Nishi M, Matsunaga S, Okamoto M, Uno M and Nishitani K 1988 Measurement of three-dimensional periodic flow on a conical draft tube at surging condition, in *Rohatgi, U. S., et al., (eds.) Flows in Non-Rotating Turbomachinery Components* FED **69** 81-88
- [4] Fanelli M A 1989 The vortex rope in the draft tube of Francis turbine operating at partial load *J Hydr Research* **27** 6 83-88
- [5] Wu Y-L, Li S, Liu S-H, Dou H-S and Qian Z-D 2013 Vibration of Hydraulic Machinery. Ch. 6 Vibration Induced by Hydraulic Excitation (*Dordrecht: Springer Verlag*)

- [6] Thicke R H 1981 Practical Solutions for Draft Tube Instability *Water Power & Dam Construction* **33** 2 31-37
- [7] Nishi M and Liu S-H 2013 An Outlook on the Draft-Tube-Surge Study *International Journal of Fluid Machinery and Systems* **6** 1 33-48
- [8] Dörfler P L, Sick M and Coutou A 2013 Flow – Induced Pulsation and Vibration in Hydroelectric Machinery. Ch. 2 Low-Frequency Phenomena in Swirling Flow (*London: Springer Verlag*)
- [9] Stuparu A and Susan-Resiga R 2015 The origin of the plunging pressure fluctuations for a swirling flow with precessing vortex rope in a straight diffuser, in *Proc. of the 6th IAHR Int. Meeting of the Workgroup on Cavitation and Dynamic Problems in Hydraulic Machinery and Systems (Ljubljana, Slovenia)* 1-8
- [10] Bosioc A, Susan-Resiga R, Muntean S and Tanasa C 2012 Unsteady pressure analysis of a swirling flow with vortex rope and axial water injection in a discharge cone, *ASME J Fluid Eng* **134** 8 081104 1-14
- [11] Tănasă C, Susan-Resiga R, Muntean S and Bosioc A 2013 Flow-feedback method for mitigating the vortex rope in decelerated swirling flows, *ASME J Fluid Eng* **135** 061304 1-12
- [12] Bosioc A, Muntean S, Tănasă C, Susan-Resiga R and Vékás L 2014 Unsteady pressure measurements of decelerated swirling flow in a draft tube cone at lower runner speeds *IOP Conf. Ser.: Earth Environ. Sci.* **22** 032008.
- [13] Javadi A, Bosioc A, Nilsson H, Muntean S and Susan-Resiga R 2016 Experimental and numerical investigation of the precessing helical vortex in a conical diffuser with rotor-stator interaction, *ASME J Fluid Eng* (accepted)
- [14] Susan-Resiga R and Muntean S 2008 Decelerated Swirling Flow Control in the Discharge Cone of Francis Turbines, in *Proc. 4th Int. Symposium on Fluid Machinery and Fluid Engineering, (Beijing, China)* 89-96
- [15] Muntean S, Bosioc A I, Stanciu R, Tănasă C and Resiga R 2011 3D Numerical Analysis of a Swirling Flow Generator, in *Proc. 4th IAHR Int. Meeting of the Workgroup on Cavitation and Dynamic Problems in Hydraulic Machinery and Systems (Belgrade, Serbia)* 115-125
- [16] Susan-Resiga R, Muntean S and Bosioc A 2008 Blade design for swirling flow generator, in *Proc. 4th German-Romanian Workshop on Turbomachinery Hydrodynamics (Stuttgart, Germany)* 1–16.
- [17] Bosioc A, Susan-Resiga R and Muntean S 2008 Design and manufacturing of a convergent-divergent test section for swirling flow apparatus, in *Proc. 4th German-Romanian Workshop on Turbomachinery Hydrodynamics (Stuttgart, Germany)* 1 - 15
- [18] Muntean S, Nilsson H and Susan-Resiga R 2009 3D numerical analysis of the unsteady turbulent swirling flow in a conical diffuser using Fluent and OpenFoam, in *Proc. 3rd IAHR Int. Meeting of the Workgroup on Cavitation and Dynamic Problems in Hydraulic Machinery and Systems (Brno, Czech Republic)* 155-165
- [19] Fluent Inc 2006 FLUENT User's guide 6.3 (*Lebanon, NH*)
- [20] Ansys Inc., 2015, FLUENT 16.1 User's Guide (*Canonsburg, PA*)
- [21] Muntean S, Tănasă C, Resiga R and Bosioc A 2015 Influence of the adverse pressure gradient on the swirling flow, in *Proc. of the Conference Modelling Fluid Flow - CMFF'15 (Budapest, Hungary)* 1 – 8
- [22] Javadi A, Bosioc A, Nilsson H, Muntean S and Susan-Resiga R 2014 Velocity and pressure fluctuations induced by the precessing helical vortex in a conical diffuser *IOP Conf. Ser.: Earth Environ. Sci.* **22** 032009 1-10
- [23] Petit O, Nilsson H, Muntean S and Susan-Resiga R 2011 Unsteady simulations of the flow in a swirl generator using OpenFOAM, *International Journal of Fluid Machinery and Systems* **4** 1 199–208
- [24] Bergman O 2010 Numerical investigation of the flow in a swirl generator, using OpenFOAM, Master Thesis, Chalmers University of Technology (*Chalmers, Sweden*)